

## Electron scattering by atomic hydrogen: Elastic and inelastic phenomena at 13.9–200 eV

Igor Bray, Dmitry A. Konovalov, and Ian E. McCarthy

*Electronic Structure of Materials Centre,  
School of Physical Sciences,  
The Flinders University of South Australia,  
G.P.O. Box 2100, Adelaide 5001, Australia*

(Received 5 June 1991)

A six-state coupled-channel optical potential method for electron-atom scattering is applied to electron-hydrogen scattering at energies of 13.87, 16.46, 19.58, 35, 40, 54.4, 100, and 200 eV. The  $n = 1, 2$ , and 3 channels are coupled explicitly, whereas the rest of the excited states of the atom including the continuum are taken into account via the *ab initio* complex nonlocal polarization potential. The differential and integrated cross sections, as well as the exchange asymmetries for  $n = 1$  and 2 channels, the total cross section, and the  $\lambda$ ,  $R$ , and  $I$  parameters for the  $2p$  excitation, are presented at each energy. The ratio of differential cross sections for  $n = 1$  to 2, and for  $2s$  to  $2p$ , and the  $2s + 2p$  differential cross sections are found to be in good agreement with experiment. There are still some discrepancies between experiment and theory for the  $2p$  angular correlation parameters  $\lambda$ ,  $R$ , and  $I$ .

PACS number(s): 34.80.Bm, 34.80.Dp, 34.80.Nz

### I. INTRODUCTION

The electron-atomic hydrogen scattering problem is an ideal testing ground for any electron-atom scattering theory; see, for instance, Refs. [1, 2]. We use the coupled-channel optical potential (CCO) method for the calculation of electron-atom scattering phenomena. This method has been recently improved [3] to cover the complete range of energies. It has been successfully applied to elastic electron scattering from atomic hydrogen [3] as well as elastic [4] and inelastic [5] electron scattering from atomic sodium at a broad range of energies.

The CCO method is an *ab initio* approach to electron-atom scattering. It treats a finite set of channels ( $P$  space) explicitly via the coupled-channel formalism, while the rest of the channels including the target continuum ( $Q$  space) are treated indirectly via the complex nonlocal polarization potential. This potential, together with the first-order potential, forms the optical potential.

The polarization potential cannot be calculated exactly, and so some approximations are used. We assume weak coupling in  $Q$  space, i.e., we omit explicit coupling between different  $Q$ -space channels. This approximation may be tested internally; see, for example, Ref. [6]. This is done by seeing the effect of including a particular channel in  $P$  space or  $Q$  space. If both results are the same, then neglecting this  $Q$ -space coupling is a good approximation. This test of approximations is only possible for discrete  $Q$ -space channels, and is not directly applicable to the continuum. As not all of the approximations may be tested internally, the complete calculations must be compared with experiment.

The aim of this paper is to present a series of 6CCO calculations ( $P = 1s, 2s, 2p, 3s, 3p, 3d$ ) at a broad range of

energies for  $n = 1, 2$  phenomena. These calculations are sufficiently convergent by the number of  $P$ -space channels since our 3CCO ( $P = 1s, 2s, 2p$ ) results are much the same as our 6CCO results. We believe that further increase in the number of  $P$ -space channels would only increase computational labor.

In Sec. II we present just the final equations used in calculating the  $T$  matrix as the complete theory can be found in Ref. [3] and references therein. In Sec. III we give the differential and integrated cross sections, spin asymmetries for the  $1s$ ,  $2s$ , and  $2p$  channels, the total cross sections, as well as the  $\lambda$ ,  $R$ , and  $I$  angular correlation parameters for the  $2p$  excitation for each considered energy. As complete agreement between our theory and experiment for elastic scattering has already been demonstrated [3, 7], we give the  $1s$  results in tabular form only for completeness. We compare our summed  $2s + 2p$ , ratio of  $n = 1$  to 2, and ratio of  $2s$  to  $2p$  differential cross sections as well as the angular correlation parameters  $\lambda$ ,  $R$ , and  $I$  with available experiments [8–20], and another *ab initio* approach to  $e$ -H scattering, the  $R$ -matrix calculations of Scholz, Walters, Burke, and Scott [2].

We find the agreement for the differential cross sections with experiment to be quite good for all considered energies. Agreement between our theory and experiment for the  $\lambda$ ,  $R$ , and  $I$  parameters is good at small to intermediate angles, but there are still some discrepancies at backward angles. It is interesting to note that there is generally good agreement between the two theories.

### II. THEORY

The Lippman-Schwinger equation for the  $T$  matrix, which depends on the total spin  $S$ , of the electron-

hydrogen scattering problem in the CCO approach is

$$\begin{aligned} \langle \mathbf{k}i | T^S | i_0 \mathbf{k}_0 \rangle &= \langle \mathbf{k}i | V_Q^S | i_0 \mathbf{k}_0 \rangle \\ &+ \sum_{i' \in P} \int d^3 k' \frac{\langle \mathbf{k}i | V_Q^S | i' \mathbf{k}' \rangle}{E^{(+)} - \varepsilon_{i'} - k'^2/2} \\ &\times \langle \mathbf{k}' i' | T^S | i_0 \mathbf{k}_0 \rangle, \end{aligned} \quad (2.1)$$

where the projectile with momentum  $\mathbf{k}_0$  is incident on the target electron in state  $i_0$  with energy  $\varepsilon_{i_0}$ , and where  $E = \varepsilon_{i_0} + k_0^2/2$  is the on-shell energy. This equation is solved in partial-wave formalism. The complete description of the method of solution may be found in Ref. [21]. By writing the coordinate space-exchange operator as  $P_r$ , the matrix elements of  $V_Q^S$  are given by [21]

$$\begin{aligned} \langle \mathbf{k}i | V_Q^S | i' \mathbf{k}' \rangle &= \langle \mathbf{k}i | v_1 + v_{12} [1 + (-1)^S P_r] | i' \mathbf{k}' \rangle \\ &+ (-1)^S \langle \mathbf{k}i | (\varepsilon_i + \varepsilon_{i'} - E) P_r | i' \mathbf{k}' \rangle \\ &+ \langle \mathbf{k}i | V_Q + (-1)^S V_Q P_r | i' \mathbf{k}' \rangle, \end{aligned} \quad (2.2)$$

where  $v_1$  is the projectile-nucleus potential and  $v_{12}$  is the projectile-target electron potential. The notation  $P$  in (2.1) indicates a finite set of discrete target states that are coupled explicitly. The remaining target states,  $Q = I - P$ , are used to calculate the matrix elements of the polarization potential operator  $V_Q$ . This operator has a complicated structure. It is nonlocal, energy dependent, and for energies above first  $Q$  channel excitation threshold it is non-Hermitian. The detailed description of the  $V_Q$  matrix elements calculation may be found in Ref. [3].

### Physical observables

Once the  $T$ -matrix elements have been obtained, a number of physical observables may be calculated. The differential cross section of the transition from  $n_0 l_0$  to  $nl$  is given by

TABLE I. Elastic differential ( $a_0^2 \text{ sr}^{-1}$ ), integrated  $\sigma_e$ , and total  $\sigma_t$  ( $\pi a_0^2$ ) cross sections calculated using the 6CCO model (see text) at a range of energies. Square brackets denote powers of 10. The semiempirical estimates of de Heer, McDowell, and Wagenaar [12] are denoted by  $\sigma^{se}$ .

E (eV)	13.87	16.46	19.58	35.0	40.0	54.4	100.0	200.0
$\theta$ (deg)								
0	1.02[1]	1.04[1]	1.02[1]	9.88	9.76	8.94	6.93	4.68
5	8.87	8.87	8.55	7.60	7.23	6.19	3.84	2.02
10	7.44	7.27	6.82	5.34	4.92	3.87	2.08	1.07
15	6.21	5.93	5.40	3.71	3.32	2.46	1.26	6.47[-1]
20	5.16	4.81	4.25	2.60	2.28	1.63	8.24[-1]	3.94[-1]
25	4.29	3.90	3.35	1.86	1.60	1.13	5.56[-1]	2.42[-1]
30	3.58	3.17	2.66	1.37	1.16	8.12[-1]	3.85[-1]	1.52[-1]
35	2.99	2.59	2.13	1.03	8.73[-1]	5.99[-1]	2.71[-1]	9.79[-2]
40	2.52	2.13	1.72	8.03[-1]	6.73[-1]	4.53[-1]	1.95[-1]	6.52[-2]
45	2.13	1.76	1.41	6.37[-1]	5.31[-1]	3.49[-1]	1.42[-1]	4.47[-2]
50	1.81	1.48	1.17	5.16[-1]	4.27[-1]	2.74[-1]	1.06[-1]	3.16[-2]
60	1.35	1.07	8.46[-1]	3.54[-1]	2.89[-1]	1.76[-1]	6.22[-2]	1.71[-2]
70	1.04	8.11[-1]	6.37[-1]	2.53[-1]	2.03[-1]	1.19[-1]	3.90[-2]	1.02[-2]
80	8.41[-1]	6.44[-1]	5.00[-1]	1.88[-1]	1.47[-1]	8.40[-2]	2.59[-2]	6.64[-3]
90	7.07[-1]	5.36[-1]	4.08[-1]	1.44[-1]	1.11[-1]	6.16[-2]	1.82[-2]	4.56[-3]
100	6.23[-1]	4.68[-1]	3.47[-1]	1.14[-1]	8.74[-2]	4.70[-2]	1.34[-2]	3.31[-3]
110	5.76[-1]	4.26[-1]	3.07[-1]	9.40[-2]	7.11[-2]	3.72[-2]	1.04[-2]	2.54[-3]
120	5.56[-1]	4.02[-1]	2.82[-1]	7.99[-2]	5.96[-2]	3.06[-2]	8.43[-3]	2.04[-3]
130	5.57[-1]	3.91[-1]	2.67[-1]	6.99[-2]	5.15[-2]	2.61[-2]	7.06[-3]	1.71[-3]
140	5.71[-1]	3.89[-1]	2.59[-1]	6.31[-2]	4.60[-2]	2.29[-2]	6.13[-3]	1.47[-3]
150	5.91[-1]	3.91[-1]	2.55[-1]	5.84[-2]	4.23[-2]	2.08[-2]	5.50[-3]	1.31[-3]
160	6.11[-1]	3.94[-1]	2.54[-1]	5.53[-2]	3.97[-2]	1.94[-2]	5.10[-3]	1.20[-3]
170	6.25[-1]	3.97[-1]	2.53[-1]	5.35[-2]	3.81[-2]	1.86[-2]	4.88[-3]	1.15[-3]
180	6.30[-1]	3.98[-1]	2.53[-1]	5.28[-2]	3.75[-2]	1.84[-2]	4.83[-3]	1.16[-3]
$\sigma_e$	5.15	4.25	3.45	1.70	1.45	1.00	0.46	0.20
$\sigma_e^{se}$			3.35±0.3		1.40±0.1		0.60±0.06	0.22±0.02
$\sigma_t$	5.93	5.42	4.81	3.42	3.24	2.85	2.06	1.28
$\sigma_t^{se}$			4.83±0.5	3.83±0.4	3.62±0.4		2.18±0.2	1.33±0.1

$$\frac{d\sigma_{nl n_0 l_0}}{d\Omega}(\theta) = \frac{(2\pi)^4 k}{(2l_0 + 1) k_0} \times \sum_S \frac{2S + 1}{4} \sum_{m, m_0} |T_{nlm n_0 l_0 m_0}^S(k, k_0, \theta)|^2, \quad (2.3)$$

where  $k_0 = \sqrt{2(E - \varepsilon_{i_0})}$ ,  $k = \sqrt{2(E - \varepsilon_i)}$ ,

$$T_{nlm n_0 l_0 m_0}^S(k, k_0, \theta) \equiv \langle \mathbf{k}i | T^S | i_0 \mathbf{k}_0 \rangle, \quad (2.4)$$

and where  $i \equiv nlm$ ,  $i_0 \equiv n_0 l_0 m_0$ , and

$$\cos \theta = \frac{\mathbf{k} \cdot \mathbf{k}_0}{kk_0}. \quad (2.5)$$

For each channel  $nl$  we can calculate the exchange asymmetry [22],  $A_{nl}$ ,

$$A_{nl}(k, k_0, \theta) = \frac{\sum_{m, m_0} |T_{nlm n_0 l_0 m_0}^0(k, k_0, \theta)|^2 - |T_{nlm n_0 l_0 m_0}^1(k, k_0, \theta)|^2}{\sum_S (2S + 1) \sum_{m, m_0} |T_{nlm n_0 l_0 m_0}^S(k, k_0, \theta)|^2}. \quad (2.6)$$

The angular correlation parameters for dipole excited channels  $\lambda$ ,  $R$ , and  $I$  (see Ref. [23] for a complete review of the subject) are given by

$$\lambda(\theta) = \frac{\sum_S (2S + 1) |T_{n10 n_0 00}^S(k, k_0, \theta)|^2}{\sum_S (2S + 1) \sum_m |T_{n1m n_0 00}^S(k, k_0, \theta)|^2}, \quad (2.7)$$

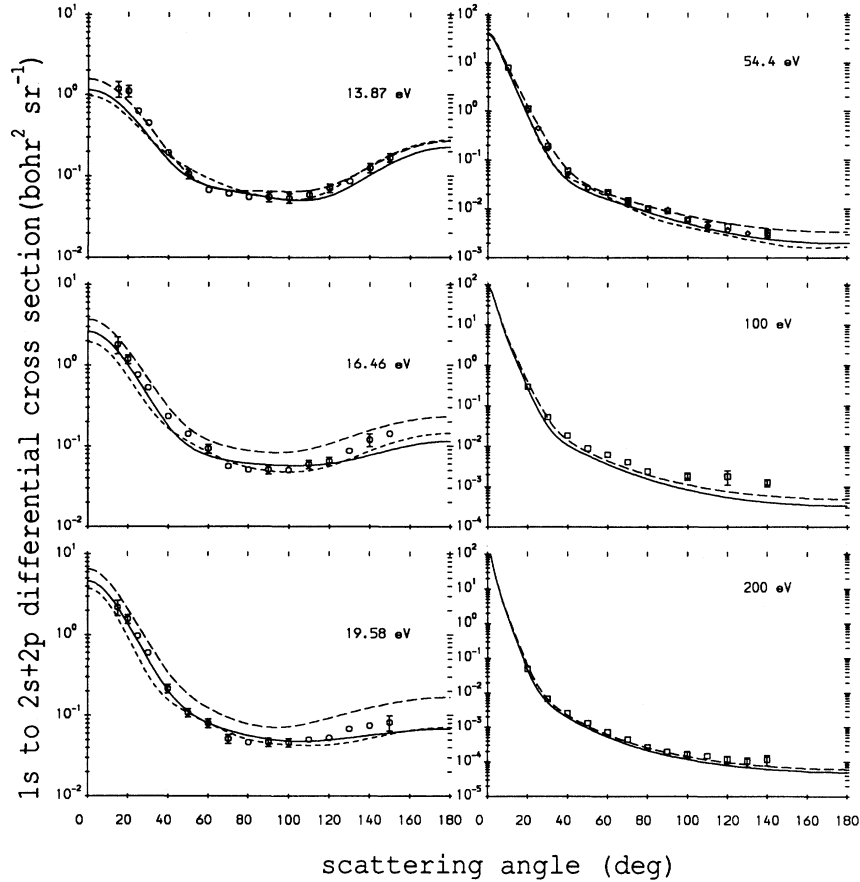


FIG. 1. The  $2s + 2p$  differential cross sections for electron scattering on atomic hydrogen. The solid line is the 6CCO calculation, the long-dashed line is the corresponding 6CC calculation, and the short-dashed line is the  $R$ -matrix calculation of [2]. The experiments of Williams [10, 17] are denoted by  $\circ$  and  $\square$ , respectively. Those of Williams and Willis [8] are denoted by  $\diamond$ . Error bars are plotted only if they are larger than the size of the symbol denoting the measurement.

$$R(\theta) = \operatorname{Re} \frac{\sum_S (2S+1) T_{n10n_000}^S(k, k_0, \theta) T_{n11n_000}^{S*}(k, k_0, \theta)}{\sum_S (2S+1) \sum_m |T_{n1m n_000}^S(k, k_0, \theta)|^2}, \quad (2.8)$$

and

$$I(\theta) = \operatorname{Im} \frac{\sum_S (2S+1) T_{n10n_000}^S(k, k_0, \theta) T_{n11n_000}^{S*}(k, k_0, \theta)}{\sum_S (2S+1) \sum_m |T_{n1m n_000}^S(k, k_0, \theta)|^2}. \quad (2.9)$$

These traditional parameters are simply related to the recently presented [23] more physical parameters  $\bar{P}_l(\theta)$ ,  $\gamma(\theta)$ ,  $L_\perp(\theta)$ , and  $P^+(\theta)$  via

$$\bar{P}_l = \sqrt{\bar{P}_1^2 + \bar{P}_2^2}, \quad (2.10)$$

$$\gamma = \arg(\bar{P}_1 + i\bar{P}_2), \quad (2.11)$$

$$L_\perp = -2\sqrt{2}I, \quad (2.12)$$

$$P^+ = \sqrt{\bar{P}_1^2 + \bar{P}_3^2}, \quad (2.13)$$

where  $\bar{P}_1$ ,  $\bar{P}_2$ , and  $\bar{P}_3$  are the reduced Stokes parameters,

$$\bar{P}_1 = 2\lambda - 1, \quad \bar{P}_2 = -2\sqrt{2}R, \quad \bar{P}_3 = 2\sqrt{2}I. \quad (2.14)$$

These, for example, describe the charge distribution of the excited  $2p$  hydrogen atom immediately after the collision as

$$|\psi|^2 \propto 1 + \bar{P}_1 \cos 2\phi + \bar{P}_2 \sin 2\phi = 1 + \bar{P}_l \cos 2(\phi - \gamma) \quad (2.15)$$

in the natural reference frame.

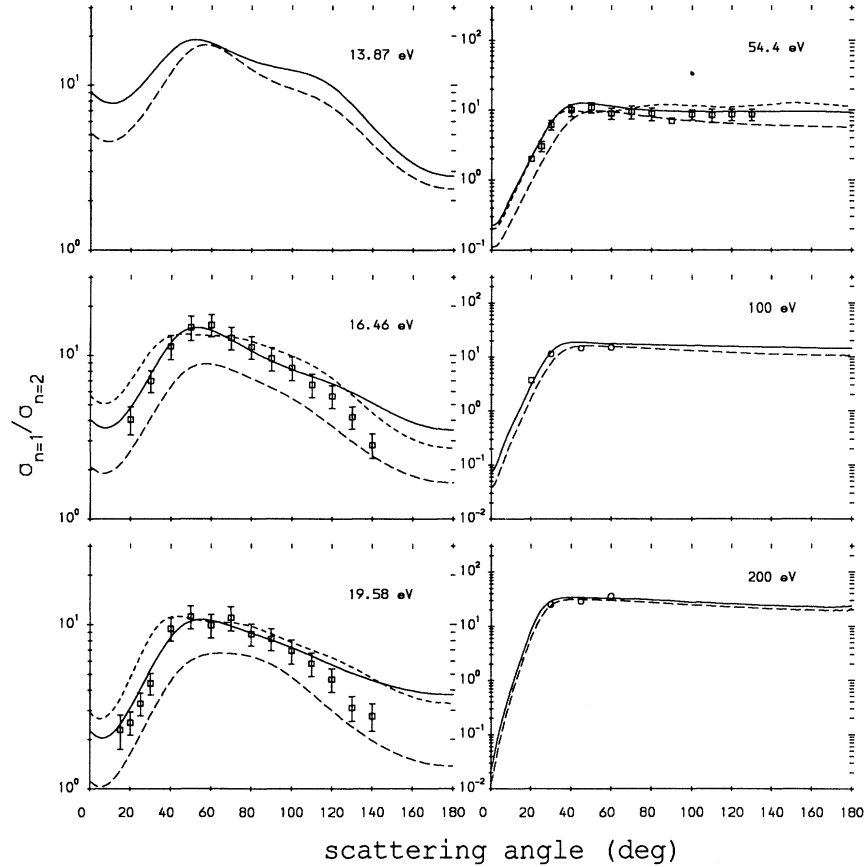


FIG. 2. The ratio of  $n = 1$  to  $2$  differential cross sections for electron scattering on atomic hydrogen. The solid line is the 6CCO calculation, the long-dashed line is the corresponding 6CC calculation, and the short-dashed line is the  $R$ -matrix calculation [2]. The direct measurements of Lower, McCarthy, and Weigold [20] are denoted by  $\circ$ . The measurements denoted by  $\square$  are derived from the elastic measurements of Callaway and Williams [11], Williams [9], and the inelastic measurements of Williams [10, 17] and Williams and Willis [8]. The 54.4-eV experimental results were obtained by interpolation of the 50- and 100-eV measurements. Error bars are plotted only if they are larger than the size of the symbol denoting the measurement.

As the measurements of angular correlation effects for electron-hydrogen scattering historically have been presented using the  $\lambda$ ,  $R$ , and  $I$  parameters we give our results using the same parameters. These may be simply converted to the new parameters using the above equations.

### III. RESULTS AND DISCUSSION

Equation (2.1) is solved with  $P$  space containing the  $1s, 2s, 2p, 3s, 3p, 3d$  channels at projectile energies ( $k_0^2/2$ ) of 13.87, 16.46, 19.58, 35, 40, 54.4, 100, and 200 eV. We denote such calculations by 6CCO. In calculating the matrix elements of  $V_Q$  in (2.2), convergence to 1% is achieved by taking in  $Q$ -space discrete states with  $n = 4, \dots, 10$ ,  $l = 0, \dots, 3$ , and 20 continuum states for each

$l = 0, \dots, 7$ . Each complete calculation takes about 24 CPU h on an IBM RISC/6000 processor. This is around 25 times longer than the 1CCO calculation, which is all that is necessary to describe elastic channel phenomena.

As we have already demonstrated excellent agreement with experiment on elastic differential cross sections [3, 7], we only present these results together with the integrated and total cross sections in Table I for completeness. In this table we also compare the integrated elastic and total cross sections with the semiempirical results of de Heer, McDowell, and Wagenaar [12], and find generally good agreement. Note that the total cross section directly tests our treatment of  $Q$  space.

In Fig. 1 we present the  $2s + 2p$  differential cross sections and compare these with experiment as well as the  $R$ -matrix calculations of Scholz *et al.* [2]. We also give the corresponding 6CC results in order to show the effect of the polarization potential. We find good agreement between experiment and theory at all considered energies

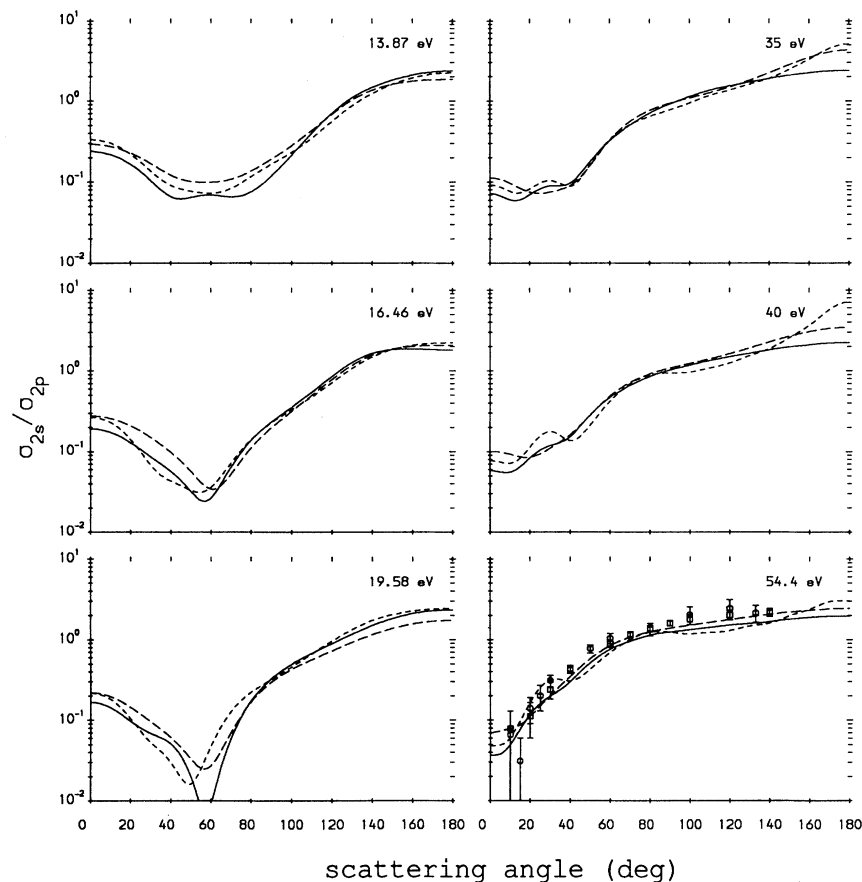


FIG. 3. The ratio of  $2s$  to  $2p$  differential cross sections for electron scattering on atomic hydrogen. The solid line is the 6CCO calculation, the long-dashed line is the corresponding 6CC calculation, and the short-dashed line is the  $R$ -matrix calculation [2]. The measurements of Frost and Weigold [15] and Williams [17] are denoted by  $\circ$  and  $\square$ , respectively.

TABLE II. The  $2s$  differential ( $a_0^2 \text{ sr}^{-1}$ ) and integrated  $\sigma_{2s}$  ( $\pi a_0^2$ ) cross sections calculated using the 6CCO model. Square brackets denote powers of 10.

E (eV)	13.87	16.46	19.58	35.0	40.0	54.4	100.0	200.0
$\theta$ (deg)								
0	2.22[-1]	4.19[-1]	6.55[-1]	1.18	1.26	1.38	1.61	1.56
5	2.06[-1]	3.82[-1]	5.79[-1]	8.15[-1]	8.21[-1]	7.47[-1]	7.11[-1]	6.22[-1]
10	1.71[-1]	2.94[-1]	4.02[-1]	3.62[-1]	3.54[-1]	3.13[-1]	3.37[-1]	2.50[-1]
15	1.27[-1]	1.94[-1]	2.32[-1]	1.59[-1]	1.62[-1]	1.58[-1]	1.52[-1]	7.42[-2]
20	8.42[-2]	1.14[-1]	1.20[-1]	7.82[-2]	8.27[-2]	8.12[-2]	6.24[-2]	2.04[-2]
25	5.08[-2]	6.23[-2]	6.11[-2]	4.05[-2]	4.27[-2]	4.00[-2]	2.54[-2]	6.66[-3]
30	2.86[-2]	3.27[-2]	3.21[-2]	2.10[-2]	2.21[-2]	2.01[-2]	1.19[-2]	3.14[-3]
35	1.59[-2]	1.74[-2]	1.78[-2]	1.13[-2]	1.26[-2]	1.17[-2]	7.10[-3]	1.83[-3]
40	9.63[-3]	9.63[-3]	1.00[-2]	7.52[-3]	9.04[-3]	8.80[-3]	5.07[-3]	1.23[-3]
45	6.92[-3]	5.44[-3]	5.16[-3]	6.72[-3]	8.32[-3]	7.89[-3]	3.92[-3]	8.48[-4]
50	5.83[-3]	3.14[-3]	2.19[-3]	7.23[-3]	8.58[-3]	7.53[-3]	3.12[-3]	6.00[-4]
60	4.82[-3]	1.95[-3]	7.18[-4]	8.93[-3]	9.15[-3]	6.73[-3]	2.02[-3]	3.25[-4]
70	4.04[-3]	3.92[-3]	3.61[-3]	9.99[-3]	8.96[-3]	5.63[-3]	1.32[-3]	1.94[-4]
80	4.18[-3]	7.33[-3]	8.23[-3]	1.01[-2]	8.16[-3]	4.51[-3]	8.94[-4]	1.24[-4]
90	5.76[-3]	1.09[-2]	1.24[-2]	9.52[-3]	7.07[-3]	3.54[-3]	6.28[-4]	8.44[-5]
100	8.95[-3]	1.48[-2]	1.59[-2]	8.68[-3]	6.07[-3]	2.82[-3]	4.66[-4]	6.24[-5]
110	1.43[-2]	2.02[-2]	1.92[-2]	7.91[-3]	5.28[-3]	2.31[-3]	3.63[-4]	4.74[-5]
120	2.34[-2]	2.76[-2]	2.33[-2]	7.25[-3]	4.69[-3]	1.95[-3]	2.96[-4]	3.87[-5]
130	3.84[-2]	3.70[-2]	2.83[-2]	6.79[-3]	4.26[-3]	1.68[-3]	2.49[-4]	3.23[-5]
140	6.11[-2]	4.73[-2]	3.38[-2]	6.53[-3]	3.98[-3]	1.51[-3]	2.19[-4]	2.82[-5]
150	9.08[-2]	5.73[-2]	3.91[-2]	6.40[-3]	3.82[-3]	1.41[-3]	2.00[-4]	2.61[-5]
160	1.23[-1]	6.57[-2]	4.35[-2]	6.35[-3]	3.73[-3]	1.34[-3]	1.88[-4]	2.35[-5]
170	1.48[-1]	7.15[-2]	4.65[-2]	6.33[-3]	3.69[-3]	1.31[-3]	1.81[-4]	2.34[-5]
180	1.58[-1]	7.35[-2]	4.75[-2]	6.34[-3]	3.70[-3]	1.31[-3]	1.76[-4]	2.18[-5]
$\sigma_{2s}$	1.16[-1]	1.14[-1]	1.09[-1]	7.21[-2]	6.70[-2]	5.45[-2]	4.14[-2]	2.51[-2]

TABLE III. The  $2p$  differential ( $a_0^2 \text{ sr}^{-1}$ ) and integrated  $\sigma_{2p}$  ( $\pi a_0^2$ ) cross sections calculated using the 6CCO model. Square brackets denote powers of 10.

E (eV)	13.87	16.46	19.58	35.0	40.0	54.4	100.0	200.0
$\theta$ (deg)								
0	9.26[-1]	2.18	3.94	1.63[1]	2.16[1]	3.78[1]	9.11[1]	2.08[2]
5	8.88[-1]	2.05	3.60	1.20[1]	1.46[1]	1.96[1]	2.05[1]	1.22[1]
10	7.88[-1]	1.70	2.81	6.00	6.37	6.32	3.89	1.36
15	6.52[-1]	1.27	1.94	2.62	2.51	2.04	8.77[-1]	1.81[-1]
20	5.09[-1]	8.88[-1]	1.24	1.12	9.96[-1]	6.92[-1]	2.12[-1]	2.72[-2]
25	3.79[-1]	5.86[-1]	7.67[-1]	4.93[-1]	4.12[-1]	2.49[-1]	5.71[-2]	5.82[-3]
30	2.75[-1]	3.79[-1]	4.69[-1]	2.35[-1]	1.87[-1]	1.01[-1]	1.94[-2]	2.14[-3]
35	1.98[-1]	2.47[-1]	2.95[-1]	1.26[-1]	9.76[-2]	4.96[-2]	9.07[-3]	1.11[-3]
40	1.46[-1]	1.68[-1]	1.96[-1]	7.81[-2]	5.92[-2]	2.93[-2]	5.42[-3]	6.87[-4]
45	1.11[-1]	1.23[-1]	1.41[-1]	5.41[-2]	4.05[-2]	1.98[-2]	3.71[-3]	4.70[-4]
50	9.03[-2]	9.79[-2]	1.10[-1]	4.10[-2]	3.02[-2]	1.46[-2]	2.70[-3]	3.39[-4]
60	7.01[-2]	7.36[-2]	7.91[-2]	2.75[-2]	1.94[-2]	8.85[-3]	1.54[-3]	2.00[-4]
70	6.18[-2]	6.15[-2]	6.14[-2]	1.99[-2]	1.36[-2]	5.87[-3]	9.61[-4]	1.27[-4]
80	5.54[-2]	5.33[-2]	4.80[-2]	1.42[-2]	9.58[-3]	3.97[-3]	6.53[-4]	9.20[-5]
90	4.86[-2]	4.74[-2]	3.82[-2]	1.02[-2]	6.92[-3]	2.85[-3]	4.80[-4]	7.02[-5]
100	4.17[-2]	4.24[-2]	3.20[-2]	7.61[-3]	5.17[-3]	2.12[-3]	3.69[-4]	5.73[-5]
110	3.60[-2]	3.73[-2]	2.84[-2]	5.81[-3]	3.96[-3]	1.63[-3]	2.96[-4]	4.79[-5]
120	3.33[-2]	3.25[-2]	2.61[-2]	4.67[-3]	3.14[-3]	1.28[-3]	2.46[-4]	4.13[-5]
130	3.51[-2]	2.93[-2]	2.42[-2]	3.95[-3]	2.59[-3]	1.06[-3]	2.11[-4]	3.67[-5]
140	4.13[-2]	2.88[-2]	2.26[-2]	3.43[-3]	2.19[-3]	9.06[-4]	1.86[-4]	3.27[-5]
150	5.02[-2]	3.13[-2]	2.14[-2]	3.07[-3]	1.93[-3]	7.89[-4]	1.70[-4]	3.08[-5]
160	5.88[-2]	3.54[-2]	2.07[-2]	2.83[-3]	1.77[-3]	7.14[-4]	1.62[-4]	2.91[-5]
170	6.47[-2]	3.90[-2]	2.04[-2]	2.68[-3]	1.67[-3]	6.74[-4]	1.59[-4]	2.84[-5]
180	6.68[-2]	4.05[-2]	2.03[-2]	2.63[-3]	1.65[-3]	6.73[-4]	1.58[-4]	2.70[-5]
$\sigma_{2p}$	3.71[-1]	4.92[-1]	6.17[-2]	6.97[-1]	7.16[-1]	7.29[-1]	6.30[-1]	4.43[-1]

other than 100 eV. However, as we get good agreement with experiment at the two adjacent energies of 54.4 and 200 eV, and there are no resonances in this region, we are not greatly concerned by this discrepancy. By comparing the 6CCO with 6CC calculations, it is interesting to note that the effect of our *ab initio* polarization potential is to reduce the differential cross section at all energies. This effect is reduced with increasing projectile energy. The quantitative differential and integrated cross sections for the  $2s$  and  $2p$  excitation may be found in Tables II and III, respectively.

The comparison between the 6CCO, 6CC, and  $R$ -matrix calculations with a number of experiments for the ratio of  $n = 1$  to 2 and the ratio of  $2s$  to  $2p$  differential cross sections may be found in Figs. 2 and 3. Some

of the experiments measured this ratio directly, whereas others were derived by taking separate measurements. Again very good agreement between the 6CCO calculations and experiment is found at each energy for which data are available.

In Figs. 4, 5, and 6 we compare, respectively, the measured angular correlation parameters  $\lambda$ ,  $R$ , and  $I$  for the  $2p$  state with the 6CCO, 6CC, and  $R$ -matrix calculations. The quantitative 6CCO results are in Tables IV – VI. We find that agreement with experiment is quite good for small to intermediate angles; however, there are still some discrepancies at some backward angles. The effect of the polarization potential is quite large for the  $\lambda$  and  $R$  parameters, and improves agreement with experiment considerably.

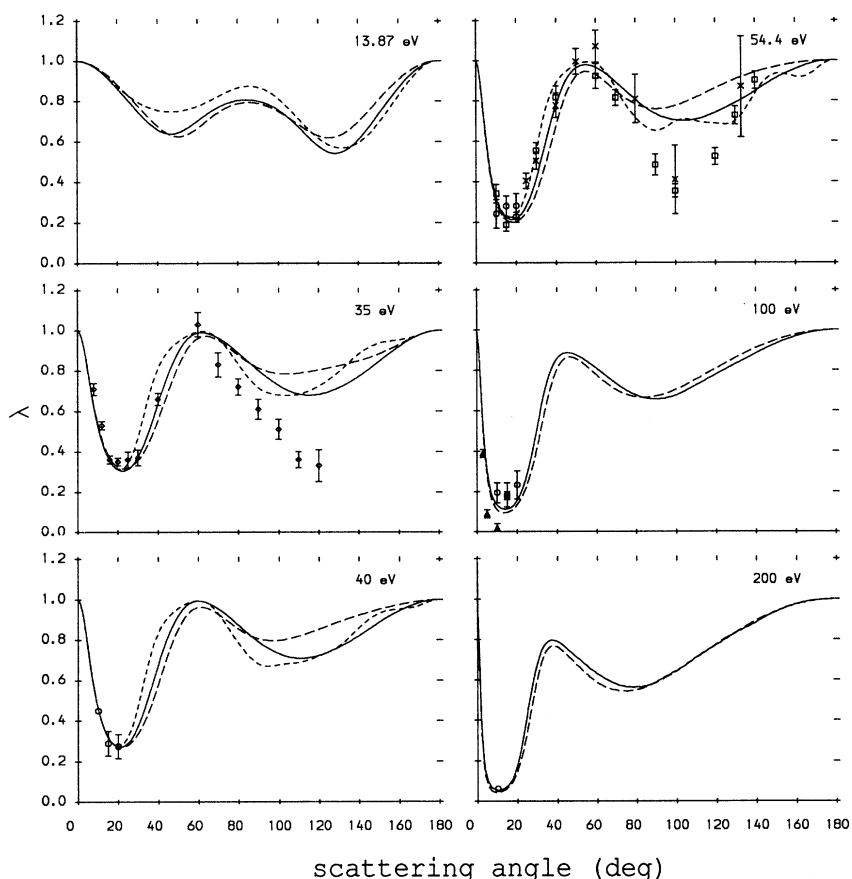


FIG. 4. The angular correlation parameter  $\lambda_{2p}$  for electron scattering on atomic hydrogen. The solid line is the 6CCO calculation, the long-dashed line is the corresponding 6CC calculation, and the short-dashed line is the  $R$ -matrix calculation [2]. The measurements of Williams [17], Hood, Weigold, and Dixon [13], Slevin *et al.* [16], Slevin *et al.* [18], and Weigold, Frost, and Nygaard [14] are denoted by  $\square$ ,  $\circ$ ,  $\diamond$ ,  $\triangle$ , and  $\times$ , respectively. Error bars are plotted only if they are larger than the size of the symbol denoting the measurement.





Unfortunately there is not a great number of measurements of the angular correlation parameters at backward angles across the energy range considered. Such measurements are very difficult as they involve the detection of photons in coincidence with the electron when the number of such electrons is very small compared to forward angles. It is interesting to note, however, that the 6CCO theory agrees reasonably well with the  $R$ -matrix theory at these angles.

As yet we have not seen any published measurements of exchange asymmetries for electron scattering on atomic hydrogen. These exist, for example, for electron scattering on atomic sodium [24]. To encourage such measurements to take place, and to make our results more comprehensive, we also present exchange asymmetries for

the  $1s$ ,  $2s$ , and  $2p$  channels in Tables VII, VIII, and IX, respectively.

#### IV. CONCLUSIONS

While our *ab initio* CCO approach to electron-atom scattering has the advantage that it uses the complete set of excited target states, is internally consistent, and is convergent by  $P$  space, the final test of the theory is by comparison with experiment. We have demonstrated complete agreement with experiment for elastic channel phenomena in our earlier work. In this paper we have demonstrated that we get generally good agreement with

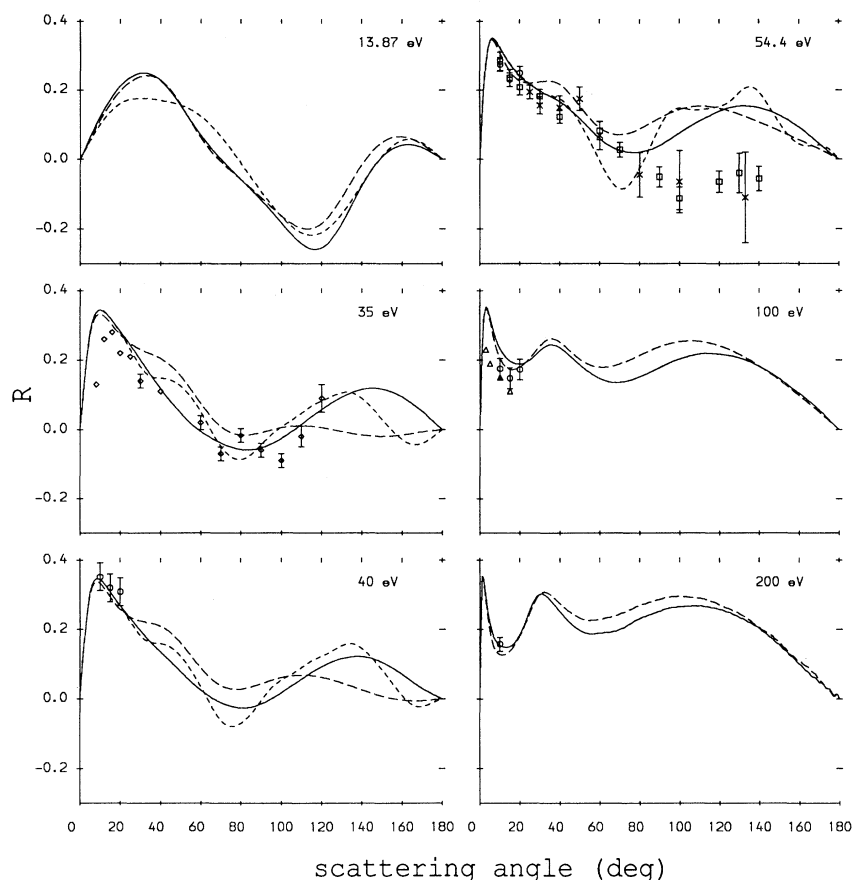


FIG. 5. The angular correlation parameter  $R_{2p}$  for electron scattering on atomic hydrogen. The solid line is the 6CCO calculation, the long-dashed line is the corresponding 6CC calculation, and the short-dashed line is the  $R$ -matrix calculation [2]. The measurements of Williams [17], Hood, Weigold, and Dixon [13], Slevin *et al.* [16], Slevin *et al.* [18], and Weigold, Frost, and Nygaard [14] are denoted by  $\square$ ,  $\circ$ ,  $\diamond$ ,  $\triangle$ , and  $\times$ , respectively. Error bars are plotted only if they are larger than the size of the symbol denoting the measurement.

TABLE VI. The angular correlation parameter  $I$  for the  $2p$  state of hydrogen calculated using the 6CCO model.

E (eV) \ $\theta$ (deg)	13.87	16.46	19.58	35.0	40.0	54.4	100.0	200.0
0	0.00	0.00	0.00	0.00	0.00	0.00	0.00	0.00
5	-0.02	-0.03	-0.04	-0.04	-0.03	-0.03	-0.02	-0.02
10	-0.05	-0.06	-0.08	-0.07	-0.07	-0.06	-0.05	-0.05
15	-0.07	-0.09	-0.11	-0.11	-0.11	-0.10	-0.10	-0.11
20	-0.10	-0.11	-0.15	-0.16	-0.16	-0.16	-0.16	-0.19
25	-0.12	-0.15	-0.18	-0.21	-0.22	-0.22	-0.24	-0.23
30	-0.15	-0.18	-0.21	-0.27	-0.27	-0.27	-0.26	-0.11
35	-0.18	-0.22	-0.25	-0.31	-0.30	-0.28	-0.18	0.03
40	-0.22	-0.26	-0.28	-0.31	-0.29	-0.22	-0.05	0.14
45	-0.25	-0.30	-0.29	-0.28	-0.24	-0.14	0.05	0.21
50	-0.28	-0.32	-0.29	-0.21	-0.16	-0.04	0.13	0.25
60	-0.30	-0.30	-0.25	-0.04	0.00	0.10	0.23	0.28
70	-0.28	-0.24	-0.18	0.08	0.12	0.21	0.28	0.28
80	-0.24	-0.17	-0.11	0.17	0.21	0.27	0.29	0.26
90	-0.20	-0.11	-0.02	0.23	0.26	0.30	0.28	0.23
100	-0.15	-0.04	0.07	0.26	0.28	0.30	0.26	0.20
110	-0.08	0.02	0.15	0.28	0.28	0.29	0.22	0.17
120	0.03	0.11	0.23	0.27	0.27	0.26	0.19	0.14
130	0.16	0.20	0.28	0.25	0.24	0.22	0.16	0.11
140	0.23	0.25	0.30	0.23	0.21	0.19	0.13	0.09
150	0.23	0.22	0.29	0.18	0.17	0.14	0.10	0.07
160	0.18	0.16	0.22	0.13	0.12	0.09	0.06	0.04
170	0.09	0.08	0.12	0.06	0.06	0.03	0.03	0.01
180	0.00	0.00	0.00	0.00	0.00	0.00	0.00	0.00

TABLE VII. The elastic exchange asymmetry  $A_{1s}$  of electron scattering on hydrogen calculated using the 6CCO model. Square brackets denote powers of 10.

E (eV) \ $\theta$ (deg)	13.87	16.46	19.58	35.0	40.0	54.4	100.0	200.0
0	-1.41[-1]	-1.24[-1]	-1.27[-1]	-7.39[-2]	-5.73[-2]	-3.60[-2]	-2.46[-2]	-2.39[-2]
5	-1.52[-1]	-1.33[-1]	-1.36[-1]	-8.17[-2]	-6.33[-2]	-3.81[-2]	-2.65[-2]	-3.80[-2]
10	-1.64[-1]	-1.46[-1]	-1.49[-1]	-9.53[-2]	-7.54[-2]	-4.89[-2]	-4.52[-2]	-6.05[-2]
15	-1.77[-1]	-1.59[-1]	-1.62[-1]	-1.13[-1]	-9.39[-2]	-6.91[-2]	-7.12[-2]	-7.22[-2]
20	-1.90[-1]	-1.73[-1]	-1.77[-1]	-1.36[-1]	-1.18[-1]	-9.59[-2]	-9.53[-2]	-7.50[-2]
25	-2.02[-1]	-1.87[-1]	-1.92[-1]	-1.62[-1]	-1.45[-1]	-1.25[-1]	-1.13[-1]	-7.36[-2]
30	-2.13[-1]	-2.01[-1]	-2.07[-1]	-1.89[-1]	-1.74[-1]	-1.53[-1]	-1.25[-1]	-7.11[-2]
35	-2.24[-1]	-2.15[-1]	-2.22[-1]	-2.13[-1]	-2.00[-1]	-1.77[-1]	-1.33[-1]	-6.89[-2]
40	-2.33[-1]	-2.29[-1]	-2.36[-1]	-2.35[-1]	-2.22[-1]	-1.95[-1]	-1.36[-1]	-6.68[-2]
45	-2.42[-1]	-2.41[-1]	-2.49[-1]	-2.51[-1]	-2.39[-1]	-2.08[-1]	-1.37[-1]	-6.41[-2]
50	-2.49[-1]	-2.52[-1]	-2.61[-1]	-2.63[-1]	-2.50[-1]	-2.16[-1]	-1.36[-1]	-6.06[-2]
60	-2.59[-1]	-2.70[-1]	-2.80[-1]	-2.74[-1]	-2.60[-1]	-2.20[-1]	-1.29[-1]	-5.24[-2]
70	-2.63[-1]	-2.80[-1]	-2.89[-1]	-2.71[-1]	-2.56[-1]	-2.13[-1]	-1.18[-1]	-4.57[-2]
80	-2.60[-1]	-2.82[-1]	-2.88[-1]	-2.56[-1]	-2.41[-1]	-1.96[-1]	-1.05[-1]	-4.08[-2]
90	-2.48[-1]	-2.72[-1]	-2.74[-1]	-2.30[-1]	-2.17[-1]	-1.74[-1]	-9.06[-2]	-3.61[-2]
100	-2.25[-1]	-2.49[-1]	-2.48[-1]	-1.96[-1]	-1.84[-1]	-1.46[-1]	-7.63[-2]	-3.17[-2]
110	-1.91[-1]	-2.12[-1]	-2.10[-1]	-1.56[-1]	-1.45[-1]	-1.17[-1]	-6.22[-2]	-2.75[-2]
120	-1.50[-1]	-1.63[-1]	-1.64[-1]	-1.15[-1]	-1.05[-1]	-8.82[-2]	-4.82[-2]	-2.25[-2]
130	-1.09[-1]	-1.06[-1]	-1.14[-1]	-7.77[-2]	-7.13[-2]	-6.04[-2]	-3.54[-2]	-1.89[-2]
140	-7.39[-2]	-5.06[-2]	-6.46[-2]	-4.61[-2]	-4.42[-2]	-3.60[-2]	-2.49[-2]	-1.82[-2]
150	-4.61[-2]	-7.04[-4]	-2.03[-2]	-2.12[-2]	-2.06[-2]	-1.65[-2]	-1.73[-2]	-1.85[-2]
160	-2.70[-2]	3.77[-2]	1.41[-2]	-1.96[-3]	3.51[-3]	-1.86[-3]	-1.27[-2]	-1.67[-2]
170	-1.60[-2]	6.17[-2]	3.60[-2]	1.14[-2]	2.48[-2]	7.79[-3]	-1.07[-2]	-1.22[-2]
180	-1.23[-2]	7.01[-2]	4.36[-2]	1.68[-2]	3.43[-2]	1.17[-2]	-9.47[-3]	-9.87[-3]

TABLE VIII. The exchange asymmetry  $A_{2s}$  for the  $2s$  excitation of hydrogen by electron scattering calculated using the 6CCO model. Square brackets denote powers of 10.

$\theta$ (deg)	E (eV)	13.87	16.46	19.58	35.0	40.0	54.4	100.0	200.0
0		1.38[-1]	1.49[-1]	1.27[-1]	1.47[-1]	1.33[-1]	9.51[-2]	3.14[-2]	6.24[-3]
5		1.42[-1]	1.54[-1]	1.35[-1]	1.72[-1]	1.56[-1]	1.15[-1]	3.27[-2]	8.77[-3]
10		1.53[-1]	1.69[-1]	1.56[-1]	2.22[-1]	1.89[-1]	1.11[-1]	2.99[-2]	2.62[-2]
15		1.73[-1]	1.91[-1]	1.89[-1]	2.35[-1]	1.70[-1]	6.91[-2]	4.79[-2]	6.18[-2]
20		2.02[-1]	2.18[-1]	2.23[-1]	1.85[-1]	1.13[-1]	4.03[-2]	8.52[-2]	9.58[-2]
25		2.45[-1]	2.37[-1]	2.37[-1]	1.16[-1]	6.26[-2]	3.83[-2]	1.14[-1]	8.44[-2]
30		3.04[-1]	2.33[-1]	2.03[-1]	6.63[-2]	3.75[-2]	4.91[-2]	9.32[-2]	3.20[-2]
35		3.83[-1]	1.96[-1]	1.23[-1]	4.20[-2]	2.79[-2]	3.81[-2]	3.84[-2]	4.79[-3]
40		4.81[-1]	1.49[-1]	2.88[-2]	1.95[-2]	4.73[-3]	-1.90[-3]	4.73[-3]	4.70[-3]
45		5.82[-1]	1.59[-1]	-5.04[-2]	-1.55[-2]	-2.74[-2]	-3.28[-2]	1.63[-3]	1.60[-2]
50		6.80[-1]	3.13[-1]	-1.02[-1]	-3.63[-2]	-4.01[-2]	-3.77[-2]	1.29[-2]	2.95[-2]
60		8.84[-1]	6.96[-1]	-2.62[-1]	-1.34[-2]	-7.62[-3]	-2.72[-3]	4.08[-2]	4.16[-2]
70		9.71[-1]	1.75[-1]	-3.19[-1]	2.75[-2]	3.97[-2]	4.36[-2]	7.06[-2]	5.73[-2]
80		6.50[-1]	-9.68[-2]	-3.04[-1]	5.63[-2]	7.47[-2]	8.72[-2]	1.04[-1]	8.13[-2]
90		2.23[-1]	-1.54[-1]	-2.33[-1]	8.91[-2]	1.12[-1]	1.32[-1]	1.33[-1]	8.98[-2]
100		7.21[-2]	-7.66[-2]	-9.27[-2]	1.35[-1]	1.58[-1]	1.79[-1]	1.54[-1]	9.03[-2]
110		1.35[-1]	8.11[-2]	1.00[-1]	1.97[-1]	2.15[-1]	2.23[-1]	1.74[-1]	9.22[-2]
120		2.76[-1]	2.49[-1]	2.91[-1]	2.79[-1]	2.89[-1]	2.78[-1]	1.93[-1]	1.03[-1]
130		4.05[-1]	3.89[-1]	4.39[-1]	3.75[-1]	3.76[-1]	3.39[-1]	2.15[-1]	1.13[-1]
140		4.88[-1]	4.93[-1]	5.37[-1]	4.62[-1]	4.56[-1]	3.85[-1]	2.30[-1]	1.12[-1]
150		5.30[-1]	5.66[-1]	5.98[-1]	5.32[-1]	5.19[-1]	4.11[-1]	2.34[-1]	1.04[-2]
160		5.47[-1]	6.14[-1]	6.34[-1]	5.89[-1]	5.74[-1]	4.46[-1]	2.42[-1]	1.09[-1]
170		5.54[-1]	6.41[-1]	6.52[-1]	6.30[-1]	6.17[-1]	4.93[-1]	2.52[-1]	1.18[-1]
180		5.55[-1]	6.49[-1]	6.59[-1]	6.44[-1]	6.33[-1]	5.14[-1]	2.71[-1]	1.32[-1]

TABLE IX. The exchange asymmetry  $A_{2p}$  for the  $2p$  excitation of hydrogen by electron scattering calculated using the 6CCO model. Square brackets denote powers of 10.

$\theta$ (deg)	E (eV)	13.87	16.46	19.58	35.0	40.0	54.4	100.0	200.0
0		2.22[-1]	1.75[-1]	1.71[-1]	2.32[-2]	2.25[-2]	1.67[-2]	6.81[-3]	1.89[-3]
5		2.28[-1]	1.81[-1]	1.77[-1]	2.29[-2]	2.31[-2]	1.91[-2]	1.29[-2]	9.77[-3]
10		2.44[-1]	1.99[-1]	1.95[-1]	2.41[-2]	2.69[-2]	2.94[-2]	3.47[-2]	3.69[-2]
15		2.72[-1]	2.30[-1]	2.28[-1]	3.01[-2]	3.81[-2]	5.21[-2]	7.40[-2]	8.12[-2]
20		3.12[-1]	2.76[-1]	2.77[-1]	4.39[-2]	5.95[-2]	8.67[-2]	1.16[-1]	1.04[-1]
25		3.66[-1]	3.36[-1]	3.43[-1]	6.39[-2]	8.57[-2]	1.18[-1]	1.18[-1]	3.45[-2]
30		4.32[-1]	4.08[-1]	4.24[-1]	8.03[-2]	9.91[-2]	1.15[-1]	4.90[-2]	-4.99[-2]
35		5.09[-1]	4.82[-1]	5.07[-1]	8.12[-2]	8.31[-2]	6.41[-2]	-3.02[-2]	-4.52[-2]
40		5.87[-1]	5.38[-1]	5.69[-1]	7.14[-2]	5.04[-2]	-3.26[-4]	-5.75[-2]	-1.24[-2]
45		6.56[-1]	5.58[-1]	5.87[-1]	6.93[-2]	3.17[-2]	-3.50[-2]	-5.14[-2]	-2.70[-4]
50		7.02[-1]	5.39[-1]	5.58[-1]	8.36[-2]	3.91[-2]	-3.33[-2]	-3.78[-2]	-8.28[-3]
60		7.15[-1]	4.60[-1]	4.27[-1]	1.21[-1]	8.29[-2]	1.44[-2]	-3.59[-4]	-7.00[-3]
70		6.80[-1]	4.22[-1]	3.19[-1]	1.19[-1]	9.73[-2]	4.96[-2]	4.42[-2]	3.30[-2]
80		6.46[-1]	4.26[-1]	2.79[-1]	9.43[-2]	9.14[-2]	7.28[-2]	6.59[-2]	5.42[-2]
90		6.16[-1]	4.30[-1]	2.93[-1]	6.84[-2]	7.97[-2]	8.50[-2]	7.27[-2]	4.60[-2]
100		5.82[-1]	4.12[-1]	3.32[-1]	6.10[-2]	7.50[-2]	8.76[-2]	7.66[-2]	4.42[-2]
110		5.45[-1]	3.78[-1]	3.70[-1]	8.50[-2]	9.45[-2]	9.96[-2]	7.72[-2]	4.80[-2]
120		5.01[-1]	3.46[-1]	4.04[-1]	1.26[-1]	1.30[-1]	1.24[-1]	7.47[-2]	4.83[-2]
130		4.38[-1]	3.21[-1]	4.46[-1]	1.62[-1]	1.56[-1]	1.30[-1]	7.51[-2]	5.03[-2]
140		3.62[-1]	2.96[-1]	5.04[-1]	1.89[-1]	1.75[-1]	1.28[-1]	7.76[-2]	5.49[-2]
150		2.91[-1]	2.63[-1]	5.71[-1]	2.06[-1]	1.90[-1]	1.34[-1]	7.96[-2]	4.94[-2]
160		2.37[-1]	2.28[-1]	6.30[-1]	2.09[-1]	1.98[-1]	1.43[-1]	7.98[-2]	4.48[-2]
170		2.03[-1]	2.03[-1]	6.68[-1]	2.00[-1]	1.90[-1]	1.31[-1]	7.21[-2]	4.67[-2]
180		1.91[-1]	1.94[-1]	6.81[-1]	1.94[-1]	1.83[-1]	1.17[-1]	7.20[-2]	3.84[-2]

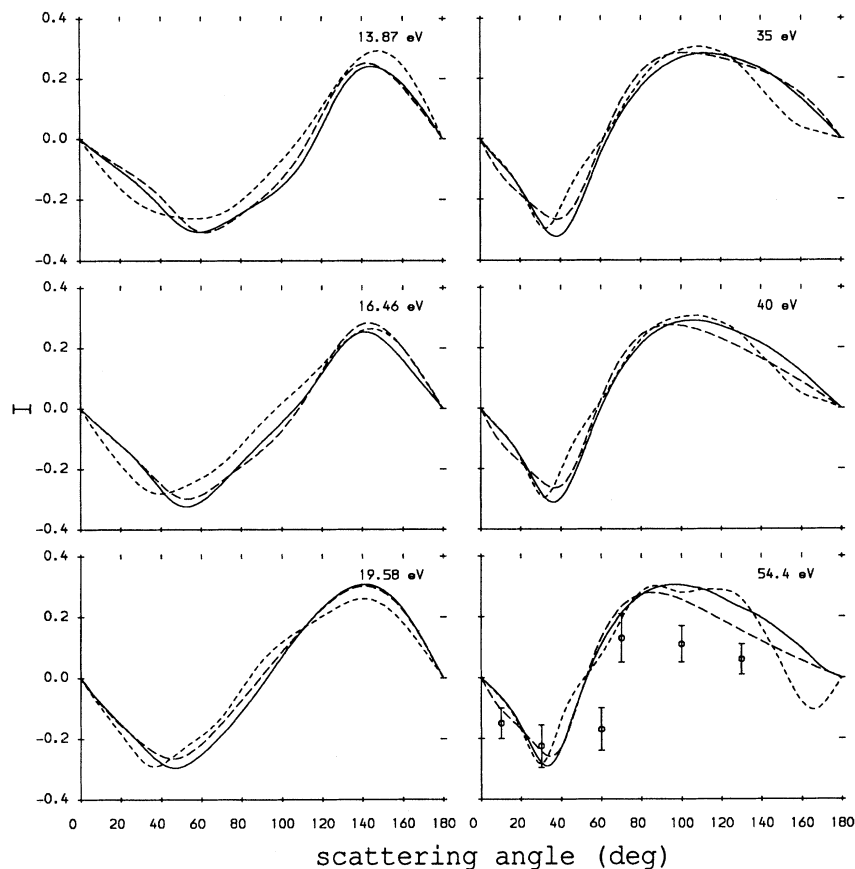


FIG. 6. The angular correlation parameter  $I_{2p}$  for electron scattering on atomic hydrogen. The solid line is the 6CCO calculation, the long-dashed line is the corresponding 6CC calculation, and the short-dashed line is the  $R$ -matrix calculation [2]. The measurements of Williams [19] are denoted by  $\circ$ .

experiment for the more sensitive  $n = 2$  inelastic phenomena.

To establish whether some of the remaining discrepancies for the angular correlation parameters are systematic it would be very useful to have a greater number of measurements available across the considered energy spectrum. Should such discrepancies prove to be systematic, further development of the theory would be necessary.

#### ACKNOWLEDGMENTS

We would like to thank Dr. P. J. O. Teubner for some useful discussions, as well as Dr. T. T. Scholz for supplying tabulations of the  $R$ -matrix results. We would like to acknowledge support from the Australian Research Council. One of us (D. A. K.) acknowledges financial support from The Flinders University of South Australia.

- 
- [1] I. Bray, D. A. Konovalov, and I. E. McCarthy, Phys. Rev. A **43**, 1301 (1991).  
 [2] T. T. Scholz, H. R. J. Walters, P. G. Burke, and M. P. Scott, J. Phys. B **24**, 2097 (1991).  
 [3] I. Bray, D. A. Konovalov, and I. E. McCarthy, Phys. Rev. A **43**, 5878 (1991).  
 [4] I. Bray, D. A. Konovalov, and I. E. McCarthy, Phys. Rev. A (to be published).  
 [5] I. Bray, D. A. Konovalov, and I. E. McCarthy, Phys. Rev. A (to be published).  
 [6] I. Bray, D. A. Konovalov, and I. E. McCarthy, J. Phys. B **24**, 2083 (1991).  
 [7] I. Bray, D. H. Madison, and I. E. McCarthy, Phys. Rev. A **41**, 5916 (1990).  
 [8] J. F. Williams and B. A. Willis, J. Phys. B **8**, 1197 (1975).  
 [9] J. F. Williams, J. Phys. B **8**, 2191 (1975).  
 [10] J. F. Williams, J. Phys. B **9**, 1519 (1976).  
 [11] J. Callaway and J. F. Williams, Phys. Rev. A **12**, 2312 (1976).  
 [12] F. J. de Heer, M. R. C. McDowell, and R. W. Wagenaar, J. Phys. B **10**, 1945 (1977).  
 [13] S. T. Hood, E. Weigold, and A. J. Dixon, J. Phys. B **12**, 631 (1979).  
 [14] E. Weigold, L. Frost, and K. J. Nygaard, Phys. Rev. A **21**, 1950 (1979).  
 [15] L. Frost and E. Weigold, Phys. Rev. Lett. **45**, 247 (1980).

- [16] J. Slevin, M. Eminyan, J. M. Woolsey, G. Vassilev, and H. Q. Porter, *J. Phys. B* **13**, L341 (1980).
- [17] J. F. Williams, *J. Phys. B* **14**, 1197 (1981).
- [18] J. Slevin, M. Eminyan, J. M. Woolsey, G. Vassilev, H. Q. Porter, C. G. Back, and S. Watkin, *Phys. Rev. A* **26**, 1344 (1982).
- [19] J. F. Williams, *Aust. J. Phys.* **39**, 621 (1986).
- [20] J. Lower, I. E. McCarthy, and E. Weigold, *J. Phys. B* **20**, 4571 (1987).
- [21] I. E. McCarthy and A. T. Stelbovics, *Phys. Rev. A* **28**, 2693 (1983).
- [22] D. H. Oza, *Phys. Rev. A* **37**, 2721 (1988).
- [23] Nils Andersen, Jean W. Gallagher, and Ingolf V. Hertel, *Phys. Rep.* **165**, 1 (1988).
- [24] J. J. McClelland, M. H. Kelley, and R. J. Celotta, *Phys. Rev. A* **40**, 2321 (1989).